Journal of Radiation and Nuclear Applications
An International Journal

http://dx.doi.org/10.18576/jrna/040208

Calculation of the Shielding Parameters of Some Natural Minerals

*Yassin A. Abdel-Razek**

Nuclear Materials Authority, Cairo. Egypt

Received: 3 Mar. 2018, Revised: 17 Apr. 2019, Accepted: 20 Apr. 2019.
Published online: 1 May 2019.

Abstract: WinXCOM was employed to calculate the mass attenuation coefficient of the natural minerals; magnetite, rutile and ilmenite for the photons of energies 0.05-3 MeV. The apparent similarity in chemical composition and close densities of the studied minerals resulted in close values of the shielding parameters of them. A wall of thickness 15cm from any of the studied minerals reduces the annual effective external dose received by the workers around the piles of monazite mineral below the recommended limit.

Keywords: Mass attenuation coefficient, Black sands, WinXCOM.

1 Introduction

With increasing use of gamma rays in different purposes such as medicine and industry along with the wide spread of nuclear power plants, it has now become necessary to study attenuation properties of various materials and compounds. Radiation shielding involves placing a shielding material between the ionizing radiations source and the worker or the environment[1]. The function of shielding is to attenuate radiation to an acceptable level, thereby affording protection for personnel, equipment, and research activities. Lead is an excellent attenuator of X-ray and gamma radiation because of its high atomic weight and mass density. Most designers and builders today are familiar with the advantages of using very high density concretes for radiation shielding. Regular well known is the excellent economy which can result from the use of normal site cast concretes with locally available aggregates when space and other factors do not absolutely demand that the desired protection be achieved within minimum dimensional limits. The effectiveness of any biological shielding material is related only to its mass and concrete has an obvious advantage in this highly specialized field of construction because of its exceptionally low cost[2].

Egyptian Black Sands contain several economic minerals, such as ilmenite, magnetite and rutile as well as zircon and monazite, which are radioactive, and may cause some hazards for the persons dealing with black sands. Test-work facilities are now going on at Abu Khashaba and Rasheed separate and concentrate black sands from the Mediterranean coast of Nile delta. Some studies concerning the radioactive emanation of these sediments and its impact on the inhabitant through air were done on Abu Khashaba beach where the main heavy mineral concentration as well as the physical dressing pilot plant of the beach sands were studied [3-4]. As an example, workers at the storing areas of radioactive minerals may receive an annual external dose of 54 (mSv) at 1m from the piles of monazite[5].

In the present study, it is intended to calculate the shielding parameters of the purified natural minerals; magnetie, rutile and ilmenite separated from the Egyptian black sands and to compare their properties to that of the regular shielding materials; lead and concrete.

2 Materials and Sources

Table 1 represents the chemical composition of magnetite[6], rutile[7], ilmenite[8] and concrete NBS[9], the densities ρ (g/cm^3) of the studied materials are; magnetite (5.15), rutile (4.25), ilmenite (4.72), concrete NBS (2.25) and lead (11.34).

The chosen γ-energies (MeV) at which the shielding parameters are calculated for the studied materials are those emitted from some regular calibration and natural sources; ^{241}Am (0.0595), ^{234}Th (0.092), ^{57}Co (0.122), ^{137}Cs (0.662), ^{60}Co (1.332, 1.173), ^{40}K (1.46) and ^{232}Th (2.614).

*Corresponding author e-mail: ya_sien@hotmai.com

Table1: Fraction by weight of the chemical composition of the chosen materials.

	magnetite	rutile	ilmenite	concrete NBS	
FeO_3	84.04		22.01	H	0.56
FeO			27.9	O	49.83
TiO_2	6.2	89.58	43.95	Na	1.71
SiO_2	3.25		0.74	Mg	0.24
Al_2O_3	2.09		1.00	Al	4.56
CaO	0.49		0.51	Si	31.58
MnO	0.62		1.17	S	0.12
Cr_2O_3	0.37		0.27	K	1.92
MgO	1.14		0.7	Ca	8.26
V_2O_3	0.42	1.91	0.175		
P_2O_5			0.28		
Nb_2O_5		0.66			
ZrO2		6.98			

3 Theoretical Aspects

During its passage through a material medium, a photon undergoes several interactions such as photoelectric absorption, coherent scattering, incoherent scattering and pair production. If a photon beam having an initial intensity I_0 penetrates the matter, it will be attenuated and its intensity decreases exponentially according to the exponential law:

$$I = I_0 \, e^{-\mu x} \quad (1)$$

or

$$I = I_0 \, e^{-(\mu/\rho)\rho x} \quad (2)$$

This is called the Beer–Lambert law, where I is the transmitted intensity, μ is the linear attenuation coefficient in cm^{-1}; ρ is the material density in g cm^{-3}, x is the thickness of the absorbing medium cm, (μ/ρ) is the mass attenuation coefficient (cm^2/g). For a chemical mixture composed of various elements and compounds as our case, the total mass attenuation coefficient of the mixture is given by authors [10-19];

$$(\mu/\rho)_t = \Sigma \, w_i \, (\mu/\rho)_I \quad (3)$$

where $(\mu/\rho)_i$ and w_i are respectively the mass attenuationcoefficient and the fractional weight of the i^{th} constituent in the mixture, $(\mu/\rho)_i$ was obtained from WinXCOM. Mass attenuation coefficients can be measured experimentally or obtained from tabulations, e.g. Hubbell and Seltzer [11]. Convenient alternatives to tabulations are computer programs, such as XCOM [20] or its Windows successor WinXCOM [21]. Using these programs one can calculate the mass attenuation coefficient as needed for any element, compound or mixture, at any energy between 1 keV and 100 GeV.

The mean free path l (cm), which is the average distance traversed by a photon between two successive events in a medium of linear attenuation coefficient μ is[1]:

$$l = 1/\mu \quad (4)$$

The half value thickness HVL, the thickness needed from a material to decease the intensity to half its initial value is obtained as follows[1]:

$$HVL = \ln(2)/\mu \quad (5)$$

Similarly, the tenth value thickness TVL, the thickness needed from a material to decease the intensity to one tenth of its initial value is obtained as follows:

$$TVL = \ln(10)/\mu \quad (6)$$

4 Results and Discussion

4.1 Mass Attenuation Coefficient

Figure 1 represents the values of mass attenuation coefficient (μ/ρ) due to the different γ-interactions with the five studied materials in the energy range 0.05-3 MeV calculated by WinXCOM. Almost, the four materials magnetite, rutile, ilmenite and concrete NBS behave in the same manner over the chosen energy interval. The values of the total mass attenuation coefficient $(\mu/\rho)_t$ with coherent scattering coincides with the values without coherent scattering indicating the minor contribution of the coherent scattering of the γ-rays in the energy range 0.05-3 MeV with the materials of magnetite, rutile, ilmenite and concrete NBS. Lead shows the same behavior with the characteristic K-edge at 82 keV of the photoelectric interaction of the energies blow 0.2 MeV.
Photoelectric interaction has low contribution in the chosen energy range with the materials magnetite, rutile, ilmenite and concrete NBS while it is the dominant process for lead at the low energies which is reflected on the values of its total mass attenuation coefficient.

Incoherent scattering interaction is the dominant process with the materials magnetite, rutile, ilmenite and concrete NBS at the energies higher than 0.2 MeV. This process has minor contribution with lead over the chosen energy range 0.05-3 MeV.

Pair production process near the nucleus appears at the energy 1.173 MeV with low values of mass attenuation coefficient (~10^{-3} cm^2/g) for the studied materials while the pair production near the electron appears at 2.614 MeV with much lower values (~10^{-5} cm^2/g). Accordingly, these two processes are omitted in the coming discussions.

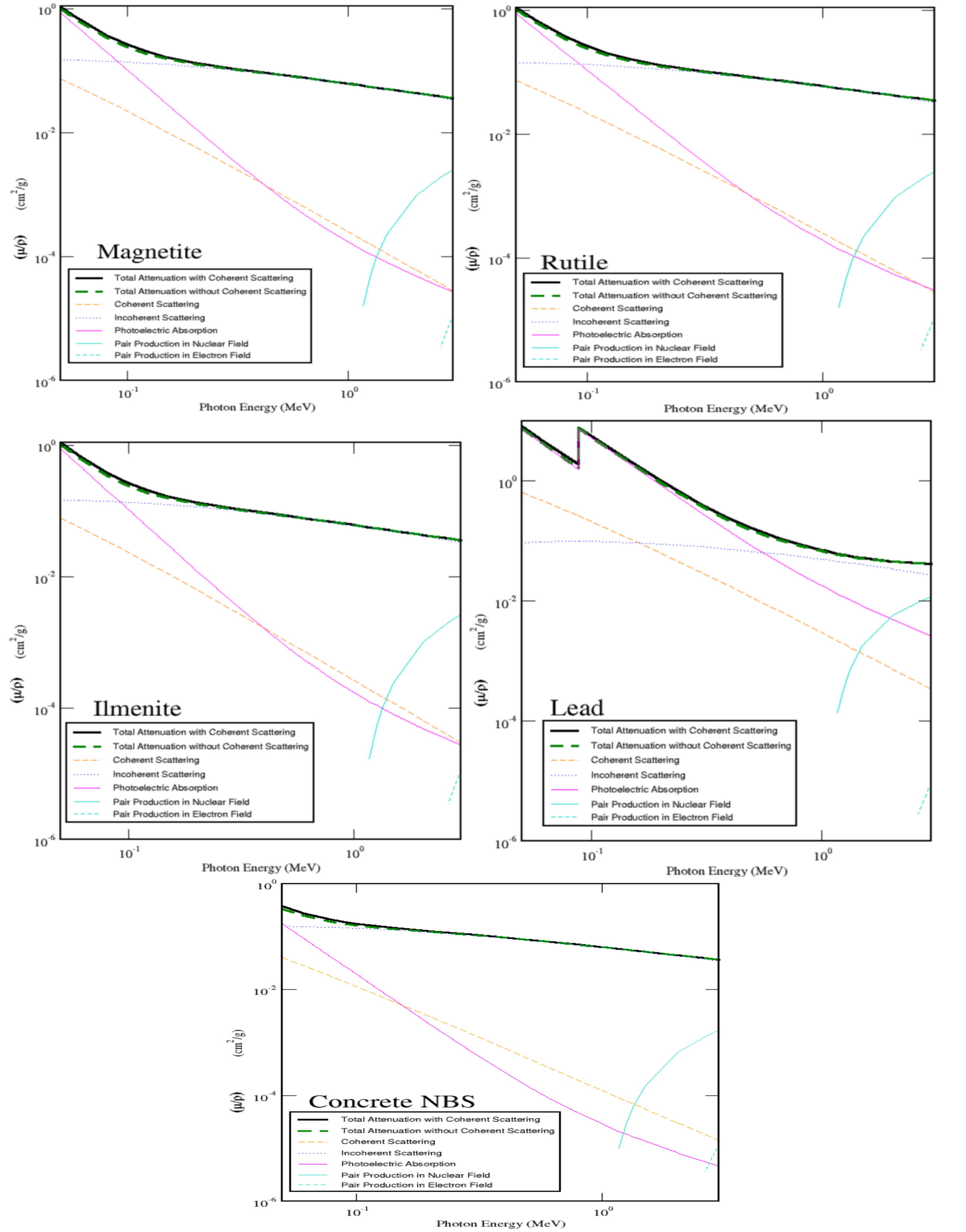

Fig. 1: Variation of the mass attenuation coefficients (μ/ρ) of the different photon interaction processes and the total mass attenuation coefficient for the studied materials over the energy range 0.05-3 (MeV) as produced by WinXCOM. The K edge (82 keV) for photoelectric interaction in lead is clarified.

To compare the response of the studied materials to photons in the energy range 0.05-3 MeV, Figure 2 represents the mass attenuation coefficients of each of the interactions; photoelectric, coherent and incoherent scattering processes along with the total mass attenuation coefficient. The three natural minerals; magnetite, rutile and ilmenite have values of mass attenuation coefficient in the same category with minimum differences.

This behavior is consistent with the almost similar chemical composition of the three minerals as shown in Table 1. This values of mass attenuation coefficient lye between the lower values of concrete NBS and the higher values of lead or vice versa. All the studied materials seem to have the same values of the total attenuation at the energies around 1.5MeV.

4.2 Shielding Parameters

To amplify the differences between the shielding properties of the studied materials, the total mass attenuation coefficient is multiplied by the density to get the linear attenuation coefficient μ. Figure 3 represents the values of the linear attenuation coefficient μ (cm^{-1}) over the energy range 0.05-3 MeV. Again, the three minerals have the moderate values of μ and lie in the same category. The values of μ for lead are higher by two orders of magnitude while concrete NBS is lower by one order of magnitude. Table 2 represents the values of μ for the materials; magnetite, rutile, ilmenite, concrete and lead at the energies emitted from the chosen calibration and natural γ-sources. Because of the K-edge for lead, the value of μ increases and decreases again.

Figure 4 represents the values of the mean free path l (cm^1) inside the studied materials over the energy range 0.05-3 MeV. According to Equation 4, this property is the inverse of μ. The higher values of l for concrete reflect the respective higher porosity of this material due its low density opposing the very low values of l that indicate the very dense element, lead. The mean free path l for the natural minerals magnetite, rutile and ilmenite has moderate values lying in the same category. Table 3 represents the values of l for the materials; magnetite, rutile, ilmenite, concrete NBS and lead at the energies emitted from the chosen calibration and natural γ-sources. Because of the edge at 82 keV for lead, the value of l decreases and increases again.

The half value layer HVL and the tenth value layer TVL are very important experimental characteristics of the shielding materials since they judge the use of the studied materials against the requirements of radiation protection. Table 4 represents the values of HVL while Table 5 represents the values TVL for the studied materials at the photon energies of the chosen sources. At all energies the three minerals; magnetite, rutile and ilmenite behave as one category between the very low values for lead and the high values for concrete NBS.

Table 2: Linear attenuation coefficient μ (cm^{-1}) of the studied materials at the energies of some frequent calibration and natural γ-sources.

Energy (MeV)	magnetite	rutile	ilmenite	lead	concrete NBS
0.0595	3.63	3.08	3.43	58.16	0.65
0.0920	1.53	1.29	1.43	77.79	0.42
0.1220	1.04	0.87	0.97	38.17	0.35
0.6620	0.39	0.31	0.36	1.25	0.17
1.1730	0.29	0.24	0.27	0.70	0.13
1.3320	0.27	0.22	0.25	0.64	0.12
1.4600	0.26	0.21	0.24	0.60	0.12
2.6140	0.20	0.16	0.18	0.49	0.09

Table 3: Mean free path l (cm) of the photons with energies of some frequent calibration and natural γ-sources inside the chosen materials.

Energy (MeV)	magnetite	rutile	ilmenite	lead	concrete NBS
0.0595	0.28	0.32	0.29	0.02	1.54
0.0920	0.65	0.78	0.70	0.01	2.39
0.1220	0.96	1.15	1.03	0.03	2.83
0.6620	2.58	3.19	2.80	0.80	5.73
1.1730	3.41	4.22	3.70	1.43	7.54
1.3320	3.64	4.50	3.95	1.57	8.04
1.4600	3.81	4.72	4.14	1.66	8.43
2.6140	5.07	6.26	5.49	2.04	11.36

Table 4: HVL (cm) of the studied materials.

Energy (MeV)	magnetite	rutile	ilmenite	lead	concrete NBS
0.0595	0.19	0.23	0.20	0.01	1.07
0.0920	0.45	0.54	0.48	0.01	1.66
0.1220	0.66	0.80	0.71	0.02	1.96
0.6620	1.79	2.21	1.94	0.56	3.97
1.1730	2.36	2.92	2.57	0.99	5.22
1.3320	2.52	3.12	2.74	1.09	5.57
1.4600	2.64	3.27	2.87	1.15	5.84
2.6140	3.51	4.34	3.80	1.42	7.87

The chosen photon energies 0.0595-2.614 MeV includes the most number of photons emitted from the elements of the radioactive series ^{238}U and ^{232}Th. Zircon and monazite minerals have elevated values of ^{238}U and ^{232}Th such that the annual external effective dose may reach 56 mSv[5].

From Table 5, a wall of thickness 15cm from any of the natural minerals; magnetite, rutile and ilmenite is estimated to reduce the annual external effective dose at 1m from this wall when used as a shield between monazite and workers down to 5.6 mSv. This meets the dose limitation recommended by the International Commision of Radiological Protection ICRP[22] that the annual effective dose received by the occupational worker shouldn't exceed 20 mSv.

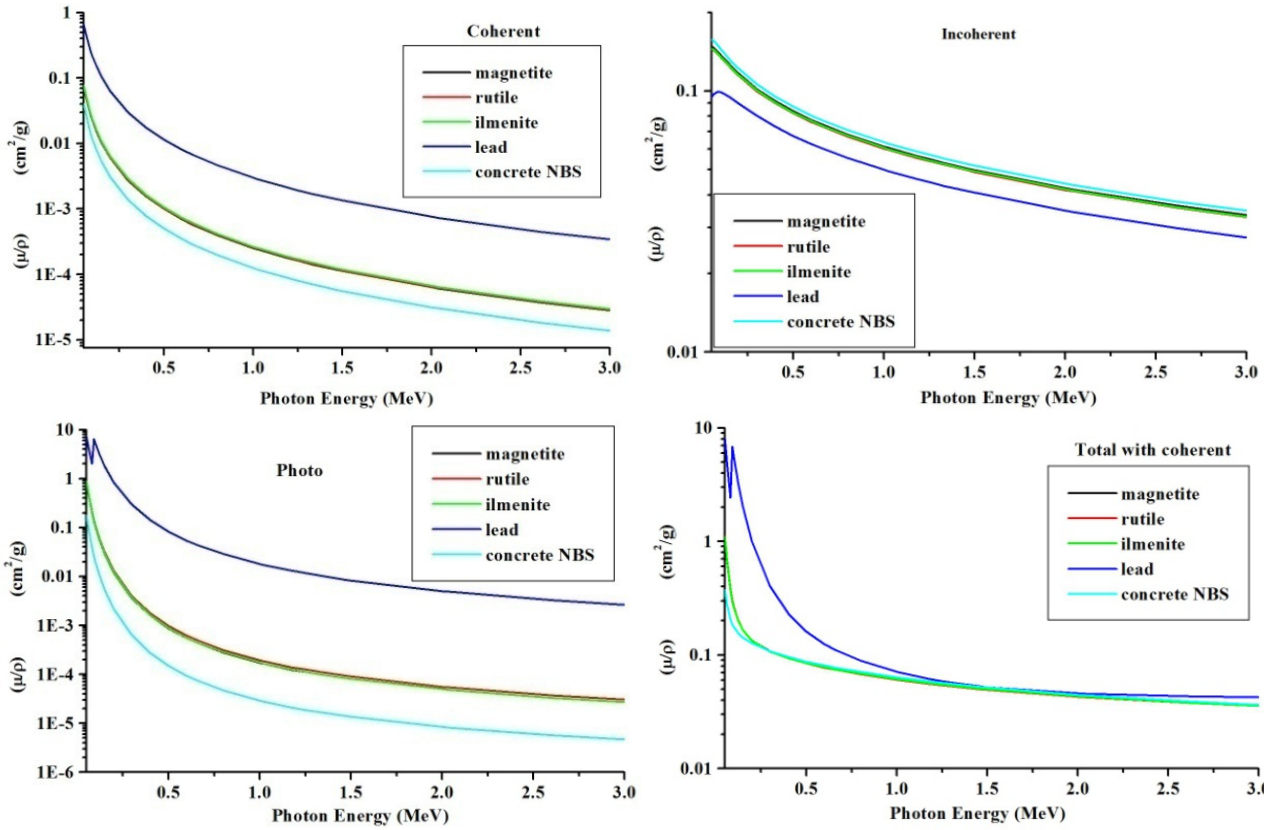

Fig. 2: Variation of the mass attenuation coefficients (μ/ρ) for the photon interactions; coherent, incoherent scattering and photoelectric processes. Also, the total mass attenuation coefficient for the studied materials over the energy range 0.05-3 (MeV) is represented.

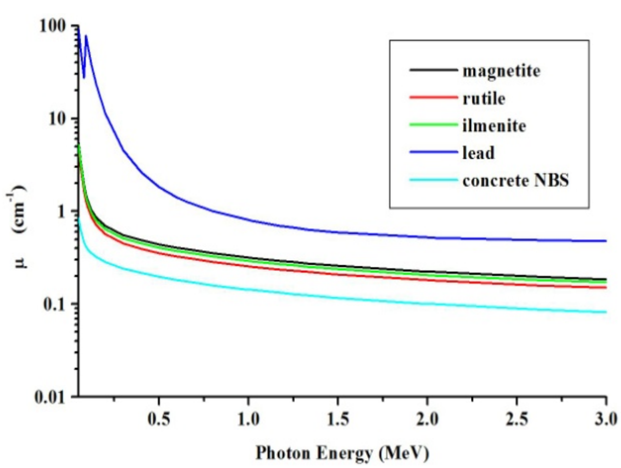

Fig.3: Linear attenuation coefficient μ (cm^{-1}) vs. photon energy (0.05-3 MeV).

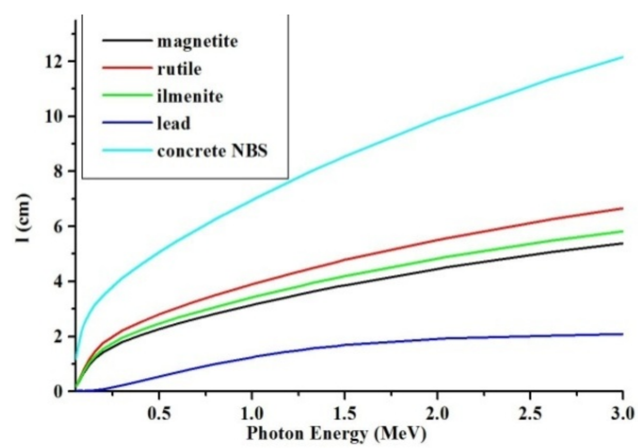

Fig.4: Mean free path l (cm) vs. photon energy (0.05-3 MeV).

Table 5: TVL (cm) of the studied materials.

Energy (MeV)	magnetite	rutile	ilmenite	lead	concrete NBS
0.0595	0.64	0.75	0.67	0.04	3.56
0.0920	1.51	1.79	1.61	0.03	5.50
0.1220	2.21	2.66	2.37	0.06	6.51
0.6620	5.94	7.35	6.46	1.84	13.20
1.1730	7.85	9.72	8.53	3.29	17.35
1.3320	8.38	10.36	9.10	3.62	18.51
1.4600	8.78	10.86	9.53	3.83	19.41
2.6140	11.66	14.42	12.63	4.70	26.16

4 Conclusions

The apparent similarity in chemical composition and close densities of the studied minerals resulted in close values of the shielding parameters of them. A wall of thickness 15cm from any of the studied minerals reduces the annual effective external dose received by the workers around the piles of monazite mineral below the recommended limit.

References

[1] S. Y. El-Kameesy, S. Abd El-Ghany, M. A. Azooz and Y. A. El-Gammam, W. J.Condens. Matt. Phys., **3**, 198-202, 2013.

[2] M. P. Ismail, N. A. Masenwat, S. Sani, A. B. Muhammad, M. K. S. Shamsuddin and R. A. Rashid https://inis.iaea.org/collection/NCLCollectionStore/_Public/44/096/44096847.pdf. 2018. Seen on Dec. 30, 2018

[3]M. S. A. Barakat: Radioactivity and Radon Emanation Measurements in Some Natural Samples. M.Sc Thesis, Faculty of Science, Menoufia University, Menoufia, Egypt, 2008.

[4] Y. A. Abdel-Razek, A. F. Said, S. F. Hassan and M. A. Elsayed, NMA-IRS-1/2012, Cairo, Egypt, 2012.

[5] Y.A. Adel-Razek, Amal S. Nasr, W. A. Khalil and M. A.Hassan https://www.researchgate.net/publication/305700279_Concentrations_of_the_airborne_radionuclides_during_the_separation_and_concentration_of_black_sands_Egypt, 2012. Seen at Dec. 30, 2018.

[6] A. M. Abdel-Karim and M. G. Barakat, Arab J. Geosci. 10, 298, 2017.

[7] A.A. El-Shennawy Arab J. Nucl. Sci. Appl., **52(1)**, 89-107, 2019.

[8] T. A. Lasheen, E.A. Saad, M.E.H. Shalabi and W. M. Abo-Elhamd, Egypt. J. Pure Appl. Sci., **53(3)**, 18–21, 2015

[9] K. S. Mann, A. Rani and M. S. Heer Radiat. Phys. Chem., **106**, 247–254, 2015.

[10] J. H. Hubbell, Phys. Med. Biol., **44(R1)**, 1999.

[11] J. H. Hubbell, S. M. Seltzer, NISTIR, 5632, 1995.

[12] J. H. Hubbell, Int. J. Appl. Radiat. Isot., **33**, 1269–1290, 1982.

[13] I. Akkurt, Ann. Nucl. Energy., **36**, 1702–1705, 2009.

[14] I. Akkurt, A. M. El-Khayatt, Ann. Nucl. Energy., **51**, 5–9, 2013.

[15] I. Akkurt, A.M.El-Khayatt, J. Radioanal. Nucl. Chem., **295**, 633–638, 2013.

[16] S. Gowda, S.K. rishnaveni, R. Gowda, Nucl. Instrum. Methods., **B 239**, 361–369, 2005.

[17] S. Gowda, S. Krishnaveni, T. Yashoda, T. K. Umesh, R. Gowda, Pramana J. Phys., **63**, 529– 541, 2004.

[18] O. Içelli, Z. Yalçina, M. Okutana, R. Boncukçuoglub, A. Sen, Ann Nucl. Energy., **38**, 2079–2085, 2011.

[19] S. R. Manohara, S. M. Hanagodimath, K. S. Thind, L. Gerward, Nucl. Instrum. Methods., **B266**, 3906–3912, 2008.

[20] M. J. Berger and J. H. Hubbell, NBSIR 87, web version 1.2, 1999.

[21] H. Singh, K. Singh, L. Gerward, H. S. Sahota and R. Nathuram, Nucl. Inst. & Methods Phys. Res. Section B: Beam Interactions with Materials and Atoms., **207(3)**, 257-262, 2003.

[22] ICRP, International Commission on Radiological Protection. ICRP Publication No. 103, Pergamon Press, Oxford and New York, 2007.